Reversible surface wettability transition between superhydrophobicity and superhydrophilicity on hierarchical micro/nanostructure ZnO mesh films

Hong Li [a,b], Maojun Zheng [a,*], Sida Liu [a], Li Ma [c], Changqing Zhu [a], Zuzhou Xiong [a]

[a] Department of Physics, Shanghai Jiao Tong University, Shanghai 200240, PR China
[b] School of Physics and Electronic Information, Huaibei Normal University, Huaibei, 235000, PR China
[c] School of Chemistry & Chemical Technology, Shanghai Jiao Tong University, Shanghai 200240, PR China

ARTICLE INFO

ABSTRACT

Large-area ZnO nanorod arrays were synthesized successfully on the stainless steel mesh through chemical vapor deposition route. The coated mesh shows good water permeability after ultraviolet (UV) irradiation, while it is impermeable to water after dark storage. This repeatable process suggests that the wettability transition of the rough surface is complete reversible. Besides, the special hierarchical nanostructures and the suitable size of the original mesh play an important role in smart controllability of the water permeability. The reversible transition of surface wettability has potential applications in many aspects, such as microchips, micro-fluidic devices, and biotechnology.

1. Introduction

In recent years, the wetting/antiwetting behavior of water droplets on solid surface has become a new research focus due to its many applications, for example, in microreactors, lab-on-chip, and small droplet manipulations [1–9]. The surface free energy and geometric structure are considered to be responsible for the wettability of solid surfaces [10–14]. Many researches [15–20] have reported the preparation of various highly water-repellent surfaces, which are usually achieved by modifying hierarchical rough surfaces with low surface energy materials, or creating nanostructures on a hydrophobic surface. Recently, with the rapid development of smart surface with controlled wetting behavior, surface wettability switching between superhydrophobicity and superhydrophilicity for the photoresponsive materials such as ZnO, WO_3, and TiO_2 has received particular attention [21].

ZnO is an important oxide semiconductor with optical band gap of 3.37 eV [22]. ZnO nanostructures, especially nanowire and nanorod, are frequently employed to acquire superhydrophobic and stimuli-responsive surfaces due to their special electrical, optical, and ultraviolet (UV)-shielding properties. Many different approaches such as sputter deposition [23], hydrothermal route [7], and chemical vapor deposition route (CVD) [24] have been used to prepare kinds of ZnO nanostructure. Among these approaches, CVD route can control the crystal structure, surface morphology, and growth rate of ZnO. So it is an idea method for ZnO nanostructure growth. Liu et al. [25] have

fabricated the ZnO thin film on the sapphire substrate through CVD route, and reversible wettability switching between superhydrophilicity and superhydrophobicity is observed via alternation of UV irradiation and dark storage. The same phenomenon is observed on the sapphire substrate coated by ZnO nanorod [26]. However, most studies focus on the wettability transition between superhydrophobicity and superhydrophilicity on different solid substrate surfaces [3,8,21,27]. The corresponding research on the wettability transition and dynamic properties for photoresponsive materials on microscale pore array is lacking [22,28]. The water permeation can be well realized by regulating the pore size of the microscale pore array. As known, the water permeation process is crucial in many aspects, such as agriculture, industry, and daily life [29–32]. The most commonly used microscale pore array is stainless steel mesh due to its wide application and easy obtainment.

In this study, we present the preparation of ZnO nanorod arrays on the stainless steel mesh through the CVD route. Reversible wettability transition between superhydrophobicity and superhydrophilicity on the coated mesh is observed, and intelligent manipulation of the reversible transition can be realized via alternation between UV irradiation and dark storage. The effects of special hierarchical nanostructures and the suitable size of the original mesh on the reversible transition were studied. This work may have very important application in many fields.

2. Experimental section

2.1. Sample preparation

A stainless steel mesh (2 cm × 5 cm) with a pore size of 75 μm was used as the substrate. The mesh was cleaned with acetone for

* Corresponding author. Tel./fax: +86 21 34202791.
E-mail addresses: lihonggreat@126.com (H. Li), mjzheng@sjtu.edu.cn (M. Zheng), lsida@163.com (S. Liu), Mali@sjtu.edu.cn (L. Ma), zhuchangqing@sjtu.edu.cn (C. Zhu), xiongzzh2010@sjtu.edu.cn (Z. Xiong).

20 min in ultrasonic bath, and then cleaned with deionized water before being dried at 80 °C for about 10 min. Then, a 50 nm thick Au film was deposited on the mesh by ion sputtering. A quartz boat filled with Zn powders (purity 99.999%) was put in the horizontal tube furnace. The mesh was placed on the downstream side of the quartz boat and the distance between the source and the mesh was about 5 cm. Subsequently, argon was introduced into the horizontal tube furnace with a flow of 120 sccm and the pressure was kept at 120 Pa. The tube furnace was heated to 650 °C at a rate of 15 °C/min and then oxygen with a flow of 80 sccm was introduced. The reaction time lasted for 40 min. After reaction, the horizontal tube furnace was cooled down to 30 °C. The wettability of the as-prepared film was measured after it was stored in the dark for 2 weeks.

2.2. Sample characterization

The surface morphologies and the structures of samples were studied by Philips Sirion 200 scanning electron microscope (SEM) and X-ray diffraction (D/max-2200/PC, XRD), respectively. The water contact angles were measured by contact angle meter system (JY-82) with liquid droplets of 5 μl. The surface chemical composition of the ZnO nanorod arrays was performed by X-ray photoelectron spectroscopy (Thermo ESCALAB 250, XPS).

3. Results and discussions

Fig. 1(a) shows the SEM image of the large area ZnO nanorod arrays on the stainless steel mesh. It can be seen that the ZnO nanorod arrays have a uniform arrangement on all stainless steel wire. Fig. 1(b) and (c) are the top surface SEM images of the ZnO nanorods at lower and higher magnification on a stainless steel wire, respectively. It can be seen in Fig. 1(b) and (c) that the ZnO nanorods exhibit a relatively uniform and densely packed distribution. Fig. 1(d) is the cross section image of the as-prepared ZnO nanorod arrays, it can be found that the ZnO nanorod arrays are almost perpendicular to the surface, and the heights of ZnO nanorods are about 4 μm. Fig. 2 indicates XRD pattern of ZnO nanorods grown on the stainless steel mesh substrate. The intensity of (002) peak is much stronger than the (100) and (101) peaks. This result indicates that ZnO nanorod arrays are highly *c*-axis oriented crystallite and perpendicular to the stainless steel mesh.
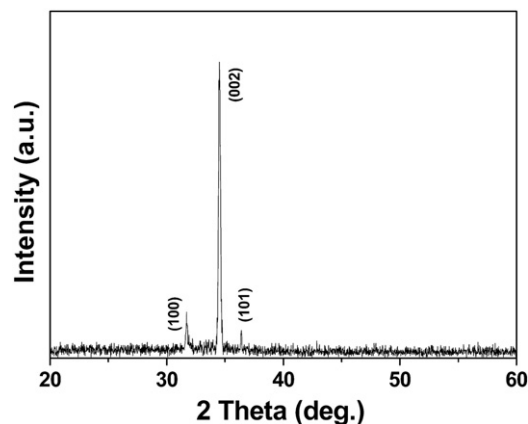

Fig. 2. XRD pattern of the as-grown ZnO nanorod arrays.

The wettability of the mesh surface which was coated by ZnO nanorod arrays was evaluated by the contact angle (CA) measurement. Fig. 3(a) depicts that the CA on this coated mesh is about 157 ± 1°. This contact angle was measured after 2 weeks of storage in the dark. However, the coated mesh shows superhydrophilicity and the CA became 0° (Fig. 3(b)) after UV irradiation (300 W Hg lamp) for 3 h, and the water will drop down when more water is added (Fig. 3(c)). The coated mesh becomes superhydrophobic after it was put in the dark for a week. The results indicate that the water permeation process can be conveniently manipulated through the alternation between UV irradiation and dark storage. Fig. 4 shows the reversible wettability switching between superhydrophilicity and superhydrophobicity.

To acquire the information about the influence of UV irradiation on the water CA of the coated mesh, the relationship between the UV irradiation time and the water CAs of the coated mesh was studied, and the results were shown in Fig. 5. The water CAs decreased sharply from 157° to 50° at the beginning of the UV irradiation time as shown in Fig. 5. However, with the increase of UV irradiation time from 60 to 180 min, the water CAs decreased only from 50° to 0°, the wettability of the coated mesh was turned into superhydrophilicity. In order to prove that the feasibility of the coated mesh can be successfully used
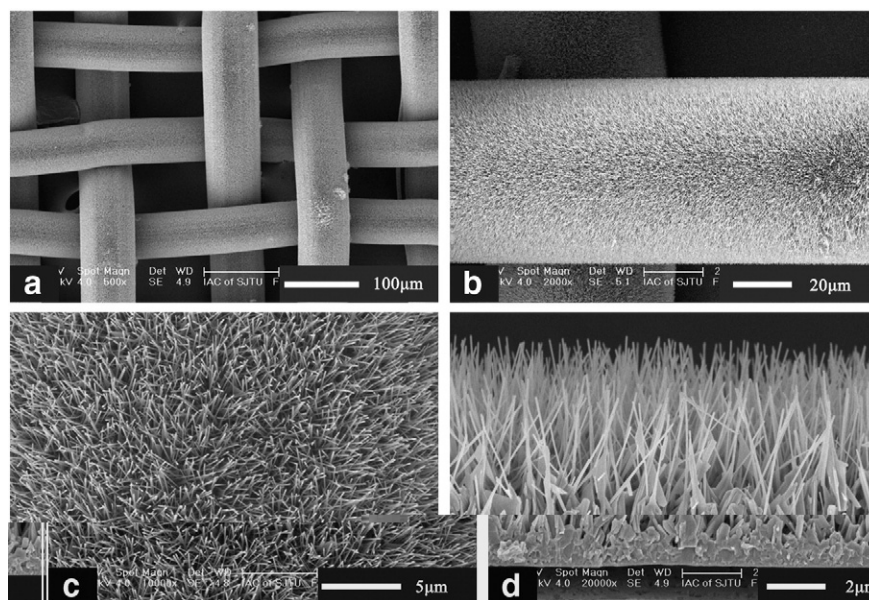

Fig. 1. SEM images of the ZnO nanorod arrays coated on the stainless steel mesh. (a) Large-area view of the coated mesh, (b) top images of the ZnO nanorods on one stainless steel wire, (c) high magnification of the as-grown ZnO nanorods, and (d) the cross section image of the ZnO nanorods with height about 4 μm.
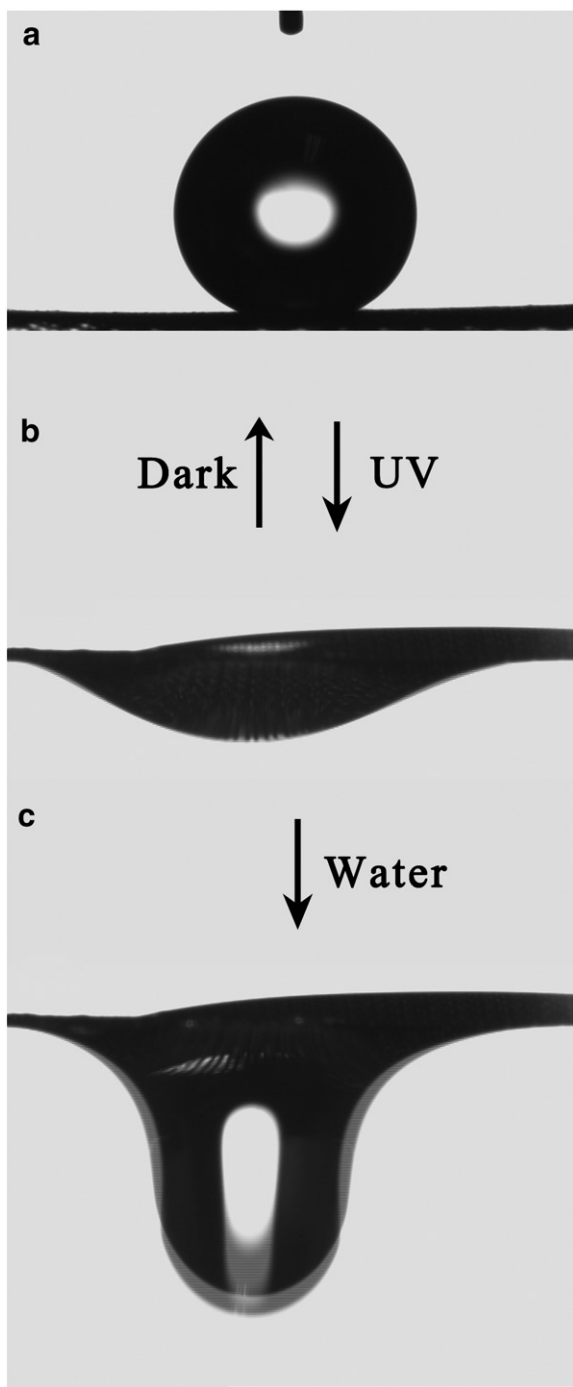
Fig. 3. Shapes of water droplets on the coated mesh. (a) Water contact angle photographs before UV irradiation, (b) after UV irradiation, and (c) permeating process of water droplet on the coated mesh after UV irradiation. When more water is dropped, the water droplet can drop down.

in practice, we design a smart device as shown in Fig. 6, a piece of coated mesh which was put in the dark for a week was fixed to the bottom of a plastic tube. Water (dyed black) cannot penetrate the coated mesh (Fig. 6(a)). However, after UV irradiation, water can quickly permeate through the coated mesh and drop into the beaker (Fig. 6(b)).

Wettability, an especially important property of solid surface, can be regulated by adjusting the surface free energy and geometric structure. Fig. 2 shows that the ZnO nanorod arrays are highly *c*-axis oriented crystal and have preferential orientation along [001] direction. Previous research results [33,34] show densities of the surface
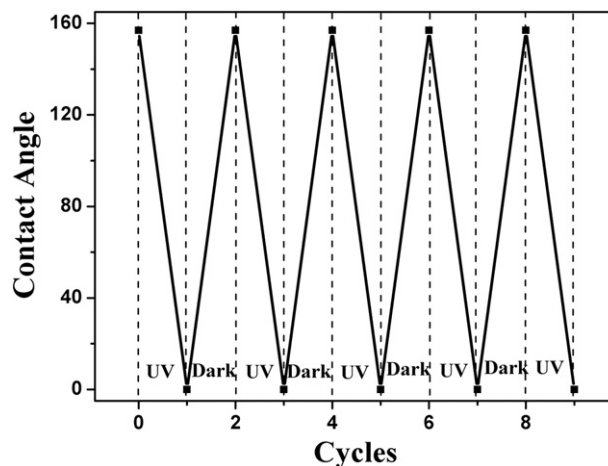

Fig. 4. Reversible wettability switching under the alternation of UV irradiation and dark storage.

free energy of the low index planes are 0.209, 0.123 and 0.009 eV/Å^2 for the (101), (110) and (002) planes, respectively. So the as-prepared ZnO nanorod arrays have the lowest surface free energy compared to other planes of ZnO nanocrystal films. In addition, there are many spaces among the different nanorods although the ZnO nanorods are densely packed as shown in Fig. 1. So ZnO nanorod arrays can trap sufficient air among the different ZnO nanorods. According to Cassie equation [35]:

$$\cos \theta^* = -1 + f_1(1 + \cos \theta) \tag{1}$$

where θ^* is contact angle of liquid droplet on the rough substrate, θ is contact angle of liquid droplet on the native flat surface, and f_1 is the fraction of solid in contact with the water droplet. Because the air has been trapped among the different ZnO nanorods, the proportions of solid/water interface decrease, then the value of f_1 diminishes quickly. The contact angle increases and the coated mesh shows the superhydrophobicity.

The wettability of solid surfaces is determined by the surface free energy and geometric structure. The geometric structure will not change after UV irradiation, which indicates that the wettability switching is caused by the changes of the surface chemical composition. ZnO is an important photocatalyst, UV irradiation generates electron-hole pairs according to Eq. (2). The formation of surface
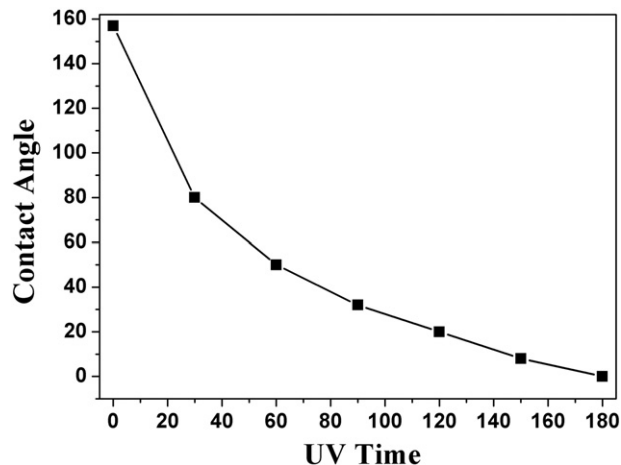

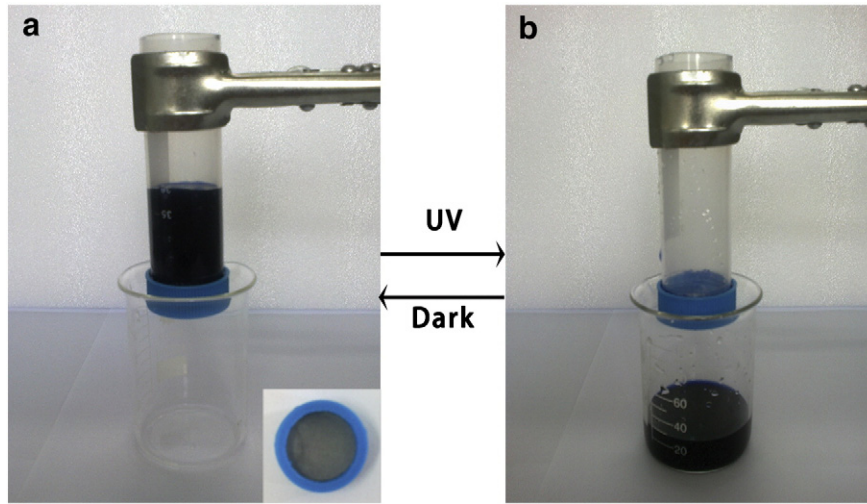**Fig. 5.** The relationship between the UV irradiation time and the water CAs of the coated mesh.

Fig. 6. Experiment process of wettability switching under the alternation of UV irradiation and dark storage. (a) Water cannot penetrate the coated mesh after dark storage, the inset is a filter holder, and (b) water can penetrate the coated mesh and dropped into the beaker.

oxygen vacancies is ascribed to the reaction between some holes and lattice oxygen as shown in Eq. (3) [36–38].

$$ZnO + 2h\nu \rightarrow 2h^+ + 2e^- \tag{2}$$

$$O^{2-} + 2h^+ \rightarrow {}^1\!/_2 O_2 + \square \quad (surface\ oxygen\ vacancy) \tag{3}$$

Meanwhile, water molecules in the air may be adsorbed on the oxygen vacancy sites, which lead to dissociative adsorption of the water molecules on the surface. To confirm the adsorption of the water molecules on the surface, the XPS measurements of ZnO nanorod arrays in the O1s peak level were carried out before and after UV irradiation as shown in Fig. 7. The increase of the shoulder and the intensity at the higher binding energy of the O1s peak shows that the adsorption of the water molecules on the surface was enhanced by UV irradiation. As a result, the ZnO nanorod arrays become hydrophilic material after UV irradiation. According to Wenzel equation [39],

$$\cos\theta^* = r\cos\theta \tag{6}$$

where r is roughness factor and the other parameters are the same as those in Eq. (1). The surface roughness increase owing to the hierarchical micro/nanostructure ZnO nanorod arrays on the mesh, and then the surface hydrophilicity is enhanced. So the coated mesh shows superhydrophilicity and the water can easily penetrate it, just like the discussion in Fig. 6(b).

Compared with the oxygen absorption, the surface oxygen vacancy sites are more favorable for hydroxyl absorption. However, the surface will become very unstable after the hydroxyl adsorption, because the hydroxyl groups distort the surface in both electronic and geometric structure. Therefore, hydroxyl groups which are adsorbed on the surface oxygen vacancy sites can be replaced gradually by oxygen atoms of the air when the superhydrophilic mesh is put in the dark. The surface wettability will evolve back to the superhydrophobicity.

Various coated mesh can be fabricated by using the original stainless steel meshes with different pore size as substrates. Fig. 8 illustrates the CAs after UV irradiation and dark storage as the function of the pore sizes which range from 25 to 600 μm. From Fig. 8, it can be found that all the coated meshes exhibit the superhydrophilicity and good water permeability under UV irradiation, while the hydrophobicity shows a considerable dependence on pore size after dark storage. The coated mesh has optimum superhydrophobicity when the pore size of the mesh is about 75 μm. The distance between the
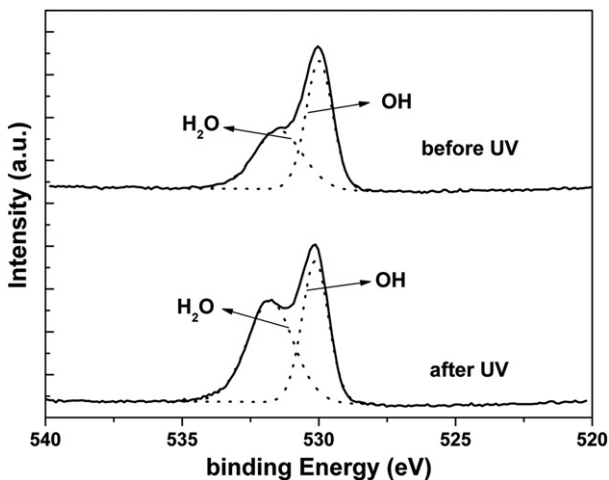

Fig. 7. X-ray photoelectron spectroscopy spectra of ZnO nanorod arrays in the O1s peak level before and after UV irradiation. Solid line, experimental data; dotted line, fitted curves.
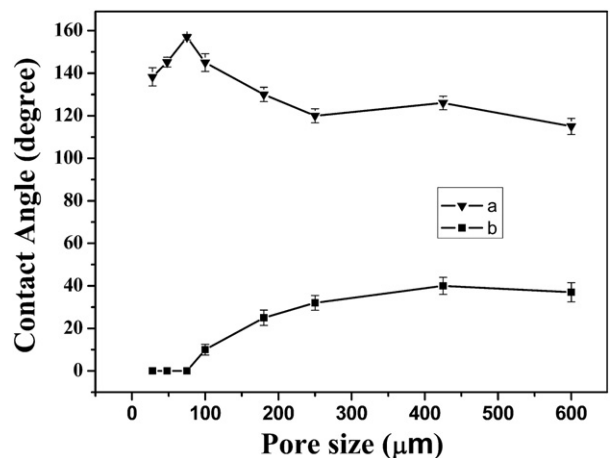

Fig. 8. The relationship between the pore sizes and the water CAs of the coated mesh. (a) After dark storage, (b) after UV irradiation.

stainless steel wires is so small that there is no insufficient proportion of the water/air interface when the pore size is below 75 μm. So the coated mesh lacks superhydrophobicity. Although at above 75 μm, the distance between the stainless steel wires is so large that micro/nanostructured stainless steel mesh cannot provide sufficient hydrophobic force. Hence, the CAs decrease as the pore size increases further. Therefore, the pore size of the original stainless steel mesh is important in achieving the reversible wettability switching of this device.

4. Conclusions

The patterned growth of ZnO nanorod arrays has been realized on the stainless steel mesh through the CVD route. The as-grown nanorod arrays are uniform in dimension and with large aspect ratios. The coated mesh is superhydrophobic and the water cannot penetrate it after dark storage, while it is superhydrophilic and the water can penetrate easily after UV irradiation. In addition, the special hierarchical nanostructures and the suitable sizes of the original mesh play an important role in the surface wettability switching between superhydrophobicity and superhydrophilicity. This work is of great significance for future industrial applications.

Acknowledgements

References

[1] A.R. Parker, C.R. Lawrence, Nature 414 (2001) 33.
[2] G. Piret, Y. Coffinier, C. Roux, O. Melnyk, R. Boukherroub, Langmuir 24 (2008) 1670.
[3] X.J. Feng, L. Feng, M.H. Jin, J. Zhai, L. Jiang, J. Am. Chem. Soc. 126 (2004) 62.
[4] N. Verplanck, E. Galopin, J.C. Camart, V. Thomy, Nano Lett. 7 (2007) 813.
[5] H.Y. Erbil, A.L. Demirel, Y. Avcl, O. Mert, Science 299 (2003) 1377.
[6] H.G. Liu, S. Szunerits, M. Pisarek, W.G. Xu, R. Boukherroub, ACS Appl. Mater. Interfaces 1 (2009) 2086.
[7] D.L. Tian, X.F. Zhang, J. Zhai, L. Jiang, Langmuir 27 (2011) 4265.
[8] M.J. Liu, X.L. Liu, C.M. Ding, Z.X. Wei, Y. Zhu, L. Jiang, Soft Matter. 7 (2011) 4163.
[9] H.Q. Liu, S. Szunerits, W.G. Xu, R. Boukherroub, ACS Appl. Mater. Interfaces 1 (2009) 1150.
[10] N. Verplanck, Y. Coffinier, V. Thomy, R. Boukherroub, Nanoscale Res. Lett. 2 (2007) 577.
[11] T. Sun, L. Feng, X. Gao, L. Jiang, Acc. Chem. Res. 38 (2005) 644.
[12] X.J. Feng, L. Jiang, Adv. Mater. 18 (2006) 3063.
[13] Y. Coffinier, S. Janel, A. Addad, R. Blossey, L. Gengembre, E. Payen, R. Boukherroub, Langmuir 23 (2007) 1608.
[14] H. Gau, S. Herminghaus, P. Lenz, R. Lipowsky, Science 283 (1999) 46.
[15] G. Perry, Y. Coffinier, V. Thomy, R. Boukherroub, Langmuir 28 (2012) 389.
[16] T. Onda, S. Shibuich, K. Tsujii, Langmuir 12 (1996) 2125.
[17] K. Tadanaga, N. Katada, T. Minami, J. Am. Ceram. Soc. 80 (1997) 1040.
[18] A. Nakajima, A. Fujishima, K. Hashimoto, T. Watanabe, Adv. Mater. 111 (1999) 1365.
[19] Z.Z. Gu, H. Uetsuka, K. Takahashi, R. Nakajima, H. Onishi, A. Fujishima, O. Sato, Angew. Chem. 42 (2003) 894.
[20] P. Brunet, F. Lapierre, V. Thomy, Y. Coffinier, R. Boukherroub, Langmuir 24 (2008) 11203.
[21] S.T. Wang, Y.L Song, L. Jiang, J. Photochem. Photobiol. C Photochem. Rev. 8 (2007) 18.
[22] J.A. Halldorsson, S.J. Little, D. Diamond, G. Spinks, G. Wallace, Langmuir 25 (2009) 11137.
[23] W. Chiou, W. Wu, J. Ting, Diamond Relat. Mater. 12 (2003) 1841.
[24] S.Y. Li, C.Y. Lee, T.Y. Tseng, J. Cryst. Growth 247 (2003) 357.
[25] H. Liu, L. Feng, J. Zhai, L. Jiang, D. Zhu, Langmuir 20 (2004) 5659.
[26] S.N. Das, J.H. choi, J.P. Kar, J.M. Myoung, Appl. Surf. Sci. 16 (2009) 7319.
[27] X.T. Zhang, O. Sato, A. Fujishima, Langmuir 20 (2004) 6065.
[28] W.L. Song, F. Xia, Y.B. Bai, F.Q. Liu, T.L. Sun, L. Jiang, Langmuir 23 (2007) 327.
[29] J. Dzubiella, J.P. Hansen, J. Chem. Phys. 122 (1) (2005) 234706.
[30] R. Allen, S. Melchionna, J.P. Hansen, Phys. Rev. Lett. 89 (1) (2002) 175502.
[31] B.L. de Groot, H. Grubmuller, Science 294 (2001) 2353.
[32] S. Sakohara, L.D. Tickanen, M.A. Anderson, J. Phys. Chem. B 96 (1992) 11086.
[33] N.H. Tran, A.J. Hartmann, R.N. Lamb, J. Phys. Chem. B 103 (1999) 4264.
[34] N. Fujimura, T. Nishihara, J. Xu, J. Cryst. Growth 130 (1993) 269.
[35] A.B.D. Cassie, S. Baxter, Trans. Faraday Soc. 40 (1944) 546.
[36] W.H. Hirschwald, Acc. Chem. Res. 18 (1985) 228.
[37] M. Miyauchi, A. Nakajima, A. Fujishima, K. Kazuhito, T. Watanabe, Chem. Mater. 12 (2000) 3.
[38] R.D. Sun, A. Nakajima, A. Fujishima, T. Watanabe, K. Hashimoto, J. Phys. Chem. B 105 (2001) 1984.
[39] R.N. Wenzel, Ind. Eng. Chem. 28 (1936) 988.